precursers, the least deviation from this angle occurs in the unoxidized precurser $NEt_3Me[Ir(CO)_2Tcbiim]$ as 7° from the perpendicular. In the other structures, this deviation averages 30°. In this respect, the NEt_3Me^+ ion seems a particularly good choice for the charge balancing cation.

Figure 7 is a perspective plot looking down the stacking axis for the mixed-metal compound. Here the cation channel is clearly visible. Cations in this channel alternate with solvent molecules. Note the uncrowded nature of the cation channel in this structure. This observation reinforces the hypothesis that insulation between cations and resulting 'comfortable space' for the cations in the lattice contributes to the overall stability of the crystal and increases its likelihood of formation. Also visible is the apparent stacking of the nitrile nitrogens. The reason for this is not clear. As it is, the interplanar distance of 3.41 Å is not far removed from the van der Waals radius of 3.46 Å estimated from the $NEt_3Me[Ir(CO)_2Tcbiim]$ structure. It is possible that at this distance the steric interactions are unimportant. The possibility of some π-cloud interaction is also suggested. All eclipsed atoms in the complex have p orbitals participating in delocalization within the complex. Other researchers have suggested this as a possibility for iridium-containing complexes with eclipsed geometry.[27]

Summary

The main body of this work has centered on the design, preparation, and structural characterization of the family of anisotropic conductors based on the planar complex $[Ir(CO)_2Tcbiim]^-$. In the course of this work, numerous new compounds have been synthesized. The conductivity of the powder forms of the compound has been improved by several orders of magnitude, and both the soluble and insoluble forms of the compound have been characterized with respect to oxidation state.

The total number of metal ion containing anisotropic conductors is small. The partially oxidized platinum cyanides and oxalates have been reviewed by Williams.[28] The metal phthalocyanines have been reviewed by Hoffman and Ibers.[29] Conducting metal thiolate complexes have been described by Cassoux et al.[30] and by Underhill.[31] In all of these systems charge is compensated as partial oxidation occurs and various structural consequences ensue. In none of them, however, is the substitution of an isoelectronic ion employed for charge compensation.

The compound $[NEt_3Me]_3[Ir(CO)_2Tcbiim]_2[Pt(CN)_2Tcbiim]$ is unique, being the first-reported one-dimensional alloy. The possibility that the electron density centered on the metal atom is nearly uniform along the stack seems likely, given the quality of the X-ray solution for this compound.

The discovery of this metal chain system has opened many possibilities for investigation of its physical properties. Previously, iridium systems have not yielded the crystals needed to bring the level of study to those cited above. The measurement of these properties is the goal of our continuing work.

Acknowledgment. P.G.R. acknowledges support from the donors of the Petroleum Research Fund, administered by the American Chemical Society. The researchers also acknowledge the assistance of William M. Butler with the crystallographic data collection.

Supplementary Material Available: Tables 1S–21S and Figures 1S–8S giving crystallographic details and unit cell views (26 pages). Ordering information is given on any current masthead page.

(27) Krogmann, K. *Z. Anorg. Allg. Chem.* **1968**, *358*, 97.

(28) Williams, Jack *Advances in Inorganic and Radiochemistry*; Emeleus, H. J., Sharpe, A. G., Eds.; Academic Press: New York, 1983; Vol. 26, pp 235–267.

(29) Hoffman, B. M.; Ibers, J. A. *Acc. Chem. Res.* **1983**, *16*, 15–21.

(30) Bousseau, M.; Valade, L.; Legros, J. P.; Cassoux, P.; Garbauskas, M.; Interrante, L. V. *J. Am. Chem. Soc.* **1986**, *108*, 1908–1916.

(31) Ahmad, M. M.; Underhill, A. *J. Chem. Soc., Dalton Trans.* **1982**, 1065–1069.

Generation and Characterization of Highly Reactive Oxo-Transfer Intermediates and Related Species Derived from (Tetraarylporphinato)manganese(III) Complexes

Kenton R. Rodgers and Harold M. Goff*

Contribution from the Department of Chemistry, University of Iowa, Iowa City, Iowa 52242.
Received March 2, 1988

Abstract: This report presents the structural and magnetic characterization of several monomeric high-oxidation-state (porphinato)manganese complexes via low-temperature NMR and ESR spectroscopies. These complexes are generated via low-temperature reaction of (porphinato)manganese(III) complexes with OCl_2, Cl_2, or *m*-chloroperoxybenzoic acid (MCPBA). The reversible redox character of these species is demonstrated by reactions with cyclohexene or iodide ion to regenerate the respective starting materials. (Tetraphenylporphinato)manganese(III) complexes (Mn(TPP)X, where X = Cl^- or OAc^-) exhibit novel reactivity with Cl_2 and OCl_2. Reaction with OCl_2 produces an axially symmetric manganese(IV) complex **1** that is thermally converted to a manganese(III) complex with loss of axial symmetry (**2**). Reaction with OCl_2 at temperatures above −78 °C results in formation of a third and axially symmetric manganese(IV) complex **3**. This complex is also ultimately converted to **2**. Complex **2** can be cleanly generated via reaction of Mn(TPP)X with Cl_2 at low temperature. However, neither **1** nor **3** can be generated by reaction with Cl_2. The presence of 4-methylpyridine in these reaction mixtures precludes formation of **2**. Low-temperature treatment of chloro(tetramesitylporphinato)manganese(III) (Mn(TMP)Cl) with OCl_2 yields the TMP analogue of **3** (**4**). A TMP analogue of **2** cannot be produced, even by reaction with Cl_2. A complex with spectroscopic properties similar to **2** (**2a**) can be generated by electrochemical oxidation. Although **2** exhibits higher reactivity than **2a**, present evidence supports tentative assignment of both complexes as isoporphyrins. Reaction of Mn(TPP)X or Mn(TMP)Cl with OCl_2 or MCPBA in the presence of hydroxide ion yields axially symmetric manganese(IV) complexes **5** and **6**, respectively. Both of these complexes react with cyclohexene or iodide ion to regenerate the respective (porphinato)manganese(III) complex.

The past decade has been witness to a multitude of studies involving transition-metal complexes that mimic the monooxygenase activity of cytochrome P-450. While reactions of high-valent iron-containing heme models have been extensively

0002-7863/88/1510-7049$01.50/0 © 1988 American Chemical Society

explored and characterized,[1] those of chromium and manganese have proven fruitful in terms of redox and/or oxygen atom transfer chemistry.[2-5] The synthetic porphyrin (especially tetraarylporphyrin) complexes of manganese have drawn particular attention. This is due in part to their facile catalytic oxygen-transfer tendencies in the presence of various reducing substrates and "classical" oxygen atom donors such as *m*-chloroperoxybenzoic acid (MCPBA) and iodosylbenzene. Further interest in the chemistry of manganese porphyrins has been fostered by their ability to effect oxygen transfer in the presence of hypochlorite ion (OCl^-), an inexpensive and readily available industrial oxidant.

Meunier et al.[3] have demonstrated the feasibility and selectivity of a biphasic system in which aqueous bleach is stirred with a CH_2Cl_2 solution of an olefin and a (porphinato)manganese(III) complex (Mn(TPP)X; X = Cl^-, Br^-, or OAc^-) in the presence of a phase-transfer catalyst. The Mn(TPP)X complex has been shown to catalyze oxygen transfer to the olefin. The result is the production of epoxides, with oxidizing equivalents being supplied by the bleach solution.

It has been shown that this biphasic reaction is more efficient, even without a phase-transfer catalyst, when the aqueous phase is more acidic than the pK_a of HOCl.[4] It has thus been suggested that a neutral chlorine(I) species can cross the H_2O/CH_2Cl_2 phase boundary and facilitate oxidation of the (porphinato)manganese(III) complex. This oxidized complex then executes a very facile oxygen transfer to the substrate. Whereas the reactivity of the putative high-valent manganese intermediate has been rather extensively characterized, the structure of said species remains elusive. It has been suggested on the basis of EXAFS and EXANES spectroscopies that the complex contains manganese(IV) bound by oxygen atoms in both axial positions.[5] We have set out to evaluate the electronic and magnetic nature of this and other high-valent (porphinato)manganese species in solution. The general approach to this investigation has been to generate the high-valent complex(es) at low temperatures without a reducing substrate present and in solvents inert toward oxidation or oxidative chlorination. The species generated were then examined via low-temperature NMR, ESR, and UV–visible spectroscopies.

The rapid hyperfine exchange and dipolar electron nuclear relaxation (and consequent line broadening) exhibited by the paramagnetic manganese complexes in this study can make acquisition of useful ^1H NMR spectra difficult or impossible. The spectral lines corresponding to ligand nuclei of paramagnetic complexes are often too broad, even at room temperature, to provide conclusive structural information. As the rate constant expressions for spin–lattice and transverse relaxation each contain a γ_1^2 term, a decrease in γ_1 manifests itself as an increase in T_1 and T_2.[6] This situation can be realized by isotopic substitution of deuterons for protons in the compound of interest. Although in principle the deuteron line should be 42 times sharper ($\gamma_D^2/\gamma_H^2 = {}^1/_{42}$) than the corresponding proton line, this resolution enhancement is rarely observed. The discrepancy is most likely due to differences in relaxation pathways for the two nuclei, namely the quadrupolar contribution to T_2 in the deuterium case. Nevertheless, deuteron NMR lines are significantly sharper than their proton counterparts in paramagnetic compounds. We have, therefore, employed specifically deuteriated porphyrin ligands for NMR experiments throughout this study. Deuteriation of the *meso*-tetraarylporphyrins at the β-pyrrole positions was particularly valuable. These ligands are relatively robust with regard to oxidative degradation. Also, the sign of the β-pyrrole deuteron hyperfine shift along with signal multiplicities can be enlightening with regard to metal ion oxidation and spin state, and molecular symmetry, respectively.[7]

We have demonstrated the utility of OCl_2 as a neutral chlorine(I) oxidant and have continued to employ it as such throughout the work described here. Previously, we reported formation of two distinct and unique oxidation products from treatment of Mn(TPP-d_8)Cl with OCl_2 at −160 °C in $CHClF_2$.[8] This report presents the follow-up to the solution characterization of these and other (tetraarylporphinato)manganese oxidation products.

Materials and Experimental Methods

H_2TPP-d_8 (β-Pyrrole-Deuteriated *meso*-Tetraphenylporphyrin). H_2TPP-d_8 was prepared according to the direct synthesis set forth by Boersma et al.[9] Chlorins were removed via column chromatography on nonactivated silica gel subsequent to metal ion insertion.[10]

H_2TPP-d_{20} (Phenyl-Deuteriated *meso*-Tetraphenylporphyrin). Perdeuteriated benzaldehyde was prepared via ceric ammonium nitrate oxidation of toluene-d_8.[11] The deuteriated benzaldehyde was utilized in the porphyrin synthesis without purification. The phenyl-deuteriated porphyrin was synthesized by allowing the benzaldehyde-d_6 to reflux with normal pyrrole in normal propionic acid as previously described.[12]

H_2TMP-d_8 (β-Pyrrole-Deuteriated *meso*-Tetramesitylporphyrin). Perdeuteriated pyrrole was prepared by shaking pyrrole with 0.1 M aqueous DCl in D_2O as described previously.[13] The pyrrole-d_5 was dried over anhydrous Na_2SO_4 and refluxed for 48 h with mesitaldehyde and anhydrous $Zn(OAc)_2$ in 2,4,6-trimethylpyridine. The product was collected and purified as previously described.[5] A CH_2Cl_2 solution of the crude product was dried over anhydrous Na_2SO_4 and refluxed with 2,3-dichloro-4,5-dicyanoquinone to oxidize the chlorins. After 2 h of reflux, the solution was passed over an alumina bed.[14] H_2TMP-d_8 was eluted from the alumina with CH_2Cl_2 and crystallized from ethanol/CH_2Cl_2. Integration of the ^1H NMR spectrum showed 17 atom % final deuterium incorporation at the β-pyrrole positions. As the pyrrole-d_5 was initially 90% enriched, it is assumed that the pyrrole and/or the porphyrin underwent isotopic exchange with the solvent during the porphyrin condensation reaction. ^1H NMR chemical shifts and electronic spectra were consistent with those previously reported.[5]

Mn(TPP-d_8)X and Mn(TMP-d_8)Cl. Manganese insertion into the porphyrins was carried out in refluxing DMF.[10] In those cases where chlorins had been previously removed, the complexes were simply crystallized from CH_2Cl_2/heptane. If chlorins had not been removed from the free-base porphyrin, the crude product was chromatographed on nonactivated silica gel. Mn(TPP-d_8)X was typically eluted with 2% methanol in dichloromethane or chloroform. After chromatographic purification, the product was crystallized from CH_2Cl_2/heptane. All (porphinato)manganese(III) complexes were dried under high vacuum at ambient temperature for 24 h. Examination of the products via silica TLC revealed only one component, and electronic spectra corresponded in all cases with those previously reported.[3,5]

(1) (a) Groves, J. T.; Watanabe, Y. *J. Am. Chem. Soc.* **1986**, *108*, 507. (b) Yuan, L.; Bruice, T. C. *J. Am. Chem. Soc.* **1986**, *108*, 1643. (c) Dicken, C. M.; Woon, T. C.; Bruice, T. C. *J. Am. Chem. Soc.* **1986**, *108*, 1636. (d) Nee, M. W.; Bruice, T. C. *J. Am. Chem. Soc.* **1982**, *104*, 6123.

(2) (a) Suslick, K. S.; Cook, B. R. *J. Chem. Soc., Chem. Commun.* **1987**, 200. (b) Collman, J. P.; Kodadek, T.; Brauman, J. I. *J. Am. Chem. Soc.* **1986**, *108*, 2588. (c) Battioni, P.; Renaud, J.; Bartoli, J. F.; Mansuy, D. *J. Chem. Soc., Chem. Commun.* **1986**, 341. (d) Renaud, J.; Battioni, P.; Bartoli, J. F.; Mansùy, D. *J. Chem. Soc., Chem. Commun.* **1985**, 888. (e) Collman, J. P.; Brauman, J. I.; Meunier, B.; Hayashi, T.; Kodadek, T.; Raybuck, S. A. *J. Am. Chem. Soc.* **1985**, *107*, 2000. (f) Yuan, L.; Bruice, T. *Inorg. Chem.* **1985**, *24*, 987. (g) Collman, J. P.; Brauman, J. I.; Meunier, B.; Raybuck, S. A.; Kodadek, T. *Proc. Natl. Acad. Sci. U.S.A.* **1984**, *81*, 3245. (h) Bortolini, O.; Meunier, B. *J. Chem. Soc., Perkin Trans. 2* **1984**, 1967. (i) Mansuy, D.; Battioni, P.; Renaud, J. *J. Chem. Soc., Chem. Commun.* **1984**, 1255. (j) Razenberg, J. A. S. J.; Nolte, R. J. M.; Drenth, W. *Tetrahedron Lett.* **1984**, *25*, 789. (k) Powell, M. F.; Pai, E. F.; Bruice, T. C. *J. Am. Chem. Soc.* **1984**, *106*, 3277. (l) Groves, J. T.; Kruper, W. R., Jr.; Haushalter, R. C. *J. Am. Chem. Soc.* **1980**, *102*, 6374.

(3) (a) Meunier, B.; Guilmet, E.; De Carvalho, M.; Poilblanc, R. *J. Am. Chem. Soc.* **1984**, *106*, 6668. (b) Meunier, B.; de Carvalho, M. E.; Bortolini, O.; Momenteau, M. *Inorg. Chem.* **1988**, *27*, 161.

(4) Montanari, F.; Penso, M.; Quici, S.; Vigano, P. *J. Org. Chem.* **1985**, *50*, 4888.

(5) Bortolini, O.; Ricci, M.; Meunier, B.; Friant, P.; Ascone, I.; Goulon, J. *Nouv. J. Chim.* **1986**, *10*, 39.

(6) McGarvey, B. R.; Kurland, R. J. In *NMR of Paramagnetic Molecules*; La Mar, G. N., Horrocks, W. D., Jr., Holm, R. H., Eds.; Academic: New York, 1973; pp 555–593.

(7) (a) La Mar, G. N.; Walker, F. A. In *The Porphyrins*; Dolphin, D., Ed.; Academic: New York, 1979; Vol. IV, pp 61–157. (b) La Mar, G. N. In *NMR of Paramagnetic Molecules*; La Mar, G. N., Horrocks, W. D., Jr., Holm, R. H., Eds.; Academic: New York, 1973; pp 85–126.

(8) Rodgers, K. R.; Goff, H. M. *J. Am. Chem. Soc.* **1987**, *109*, 611.

(9) Boersma, A. D.; Goff, H. M. *Inorg. Chem.* **1982**, *21*, 581.

(10) Adler, A. D.; Longo, F. R.; Varadi, V. *Inorg. Synth.* **1976**, *16*, 213.

(11) Fajer, J.; Borg, D. C.; Forman, A.; Felton, R. H.; Vegh, L. *Ann. N.Y. Acad. Sci.* **1973**, *206*, 349.

(12) Shirazi, A.; Goff, H. M. *J. Am. Chem. Soc.* **1982**, *104*, 6318.

(13) Miller, F. A. *J. Am. Chem. Soc.* **1942**, *64*, 1543.

(14) Fuhrhop, J. H.; Smith, K. M. *Laboratory Methods in Porphyrin and Metalloporphyrin Research*; Elsevier: Amsterdam, The Netherlands, 1975; p 14.

Mn[*N*-CH_3TPP]Cl. Chloro(*N*-methyltetraphenylporphinato)manganese(II) was prepared as prescribed by Lavallee and co-workers.[15] However, our ESR sample preparation differed as follows. Immediately before recording ESR spectra of Mn[*N*-CH_3TPP]Cl, a CH_2Cl_2 solution of the complex was shaken twice with saturated aqueous NaCl. The solution was dried over anhydrous sodium sulfate, filtered, and concentrated at room temperature under a stream of dry nitrogen in preparation for examination by ESR spectroscopy. The solution was not evaporated to dryness, as such treatment caused partial demetalation. This method of sample purification freed the solution of cubic or solvated manganese(II). Thus, the rather intense $g = 2$ signal that plagued previous ESR studies[16] of this complex was eliminated from the spectrum.

Oxidizing Agents. OCl_2 was prepared as a CCl_4 solution as previously described.[17] Due to the explosion hazard involved in further purification, the resulting OCl_2 solution was used directly for oxidation of manganese(III) complexes. Concentrations of Cl_2 and OCl_2 were determined via iodometric titrations.[17] Solutions of OCl_2 were stored in a freezer at −15 °C and protected from laboratory light.

Molecular chlorine was also utilized as an oxidant for the (porphinato)manganese(III) complexes. It was introduced as a CCl_4 solution or as a gas under anaerobic conditions using Schlenk techniques. The methods were interchangeable in terms of product formation.

Solid *m*-chloroperoxybenzoic acid (MCPBA) was purchased from a commercial vendor. The solid was shown by iodometric titration[18] to be 77% pure (by weight) at the time of use in this study. The impurities were *m*-chlorobenzoic acid and water. No attempt was made to remove the impurities. MCPBA was introduced into NMR and ESR samples as a CH_2Cl_2 solution with a gas-tight microliter syringe.

Chemical Generation of High-Valent Manganese Complexes. The general procedure for generation of the high-valent manganese complexes was to dissolve the starting material in the appropriate solvent and cool the solution to the desired temperature in dry-ice snow, dichloromethane slush, or chlorodifluoromethane (Freon 22) slush. When necessary, NMR and ESR samples were degassed in a septum-sealed tube by the freeze–pump–thaw method. The appropriately prepared sample was treated with an oxidizing agent at the desired temperature by allowing the oxidizing solution to run slowly down the side of the cold NMR or ESR tube. The solutions were mixed by shaking the tube or by bubbling cold, dry nitrogen through the solution if mixing was carried out in an ESR tube.

Electrochemical Methods. Cyclic voltammograms were recorded with a potential programmer and digital coulometer equipped with *iR* compensation capability. Bulk electrolyses were facilitated by a potentiostat with a digital coulometer to monitor cell current. Potentials were referenced to Ag/Ag^+ (silver wire immersed in 0.1 M $AgNO_3$ in CH_3CN) to avoid the large junction potential encountered with the saturated calomel electrode. However, potentials reported herein are given vs SCE. The reported potentials were calculated with an experimentally determined offset of 0.38 V vs SCE.

Cyclic voltammograms were recorded with a static solution under nitrogen in CH_2Cl_2 that was 0.1 M in Bu_4NClO_4 or Pr_4NClO_4 and 0.1 mM in porphyrin complex. The working electrode was a platinm bead, and the counter electrode consisted of a platinum wire separated from the bulk solution by a fine-porosity glass frit.

Bulk electrolyses were accomplished by holding a platinum basket electrode at the appropriate positive potential (as determined by the CV scan) until the cell current had fallen to less than 5% of its initial value. Dry nitrogen (free of water, but saturated with CH_2Cl_2) was bubbled through the solution throughout the electrolysis to facilitate stirring. The products of bulk electrolyses were concentrated at room temperature under a stream of dry nitrogen until the solutions were approximately 0.5 mM in the oxidized manganese complex. These solutions were of suitable concentration for examination by NMR and ESR spectroscopies. ^2H NMR spectral observation did not necessitate separation of the electrolysis product from protonated solvent or supporting electrolyte before the NMR experiment.

NMR Spectroscopy. ^1H NMR spectra were acquired at 360 or 300 MHz, ^2H spectra were collected at 55 or 46 MHz, and ^{13}C spectra were acquired at 90 MHz. To avoid inductive heating of the sample, ^{13}C spectra were recorded without proton decoupling. In all cases the thermocouple was calibrated in the probe used for spectral acquisition with the methanol (Van Geet) thermometer.[19]

Magnetic Susceptibility Measurements. Because manipulation of the complexes described herein often leads to decomposition and/or reduction to starting material, magnetic susceptibility was determined via Evans' NMR method.[20] In the concentric-tube configuration, the central capillary contained the reference solution, and the 5-mm tube contained the sample solution. The concentration of paramagnetic starting material was determined before generation of the high-valent species through measurement of bulk susceptibility and assumption of 4.9 μ_B as the effective magnetic moment for Mn(TPP)Cl.[21] The measurements were carried out with a solenoid magnet, hence a factor of $-2/\pi$ was included in the first term of the expression for gram susceptibility.[22] Density corrections were made in calculation of gram susceptibilities, as the solution temperature was varied over a relatively wide range. A volume coefficient for thermal expansion of 0.001 37 for CH_2Cl_2 was employed to make these corrections.[23] β-Pyrrole deuteriated porphyrins were used for magnetic susceptibility measurements as these compounds provided a means (via ^2H NMR) for demonstration of the sample integrity before and after the measurements were made.

It is worth noting that equivalent values for bulk susceptibility were obtained whether $\Delta\nu$ was measured by means of the solvent signal or the TMS signal. This indicates the lack of any significant association between solvent and metal center over the temperature range of the experiment.

Relaxation Measurements. Spin–lattice relaxation times were determined at low temperature via the method of inversion recovery. Again, the ^2H NMR spectra of the deuteriated porphyrins facilitated monitoring of sample integrity.

ESR Spectroscopy. ESR spectra were recorded at X-band (9.2 GHz) on a spectrometer equipped with a 6-kG magnet. Spectra were collected at temperatures between 5 and 80 K in a liquid-helium cryostat. Microwave powers of 2–5 mW were employed in recording derivative spectra at near-liquid-helium temperatures, whereas the corresponding rapid passage spectra were recorded at powers of 50–100 mW, and we verified in all cases that saturation was not occurring in the derivative spectra. Field modulation amplitude was typically 10 G. Derivative spectra were recorded with a field modulation frequency of 100 kHz, and modulation at the second harmonic was employed for adiabatic rapid passage experiments. Time constants and scan rates were always chosen such that sweep rate × time constant < ^{55}Mn hyperfine coupling constant (approximately 80 G). Unless otherwise specified in the text or figure legends, these parameters were employed in recording all of the ESR spectra. In cases where the potential for multiple species contributed ambiguity to spectral interpretation, sample integrity was verified by ^2H NMR.

Gas Chromatographic Analysis of Substrate Oxidation Products. Reactivities of the complexes generated in this study were probed by reaction with cyclohexene at low temperature. The products of these reactions were analyzed via gas–liquid chromatography. Separation was effected on a 10 ft × 0.125 in. Carbowax 20M column with flame ionization detection. Identification of components was facilitated by comparison of sample chromatograms with those of standards that contained known compounds.

Solvent Preparation and Purification. Dichloromethane was purified as described by Perrin, Armarego, and Perrin.[24] After distillation, CH_2Cl_2 was stored under nitrogen and over activated 4-Å molecular sieves in a refrigerator.

Chlorodifluoromethane was condensed in a liquid-nitrogen trap. The liquid was held at −78 °C in dry-ice snow. Transfer of $CHClF_2$ and $CHClF_2$ solutions (or any other solutions that had to be kept cold) between vessels was accomplished with pipets that had been precooled in liquid nitrogen.

Results

Chemistry of Mn(TPP)X with OCl_2 and Cl_2. Treatment of Mn(TPP-d_8)X with OCl_2 at −78 °C results in formation of several oxidized (porphinato)manganese complexes. The formation of these species is reversible insofar as they can be reverted to a five-coordinate (porphinato)manganese(III) complex {Mn(TPP-d_8)X} by addition of a reducing agent such as cyclohexene or iodide ion. This is easily verified via the UV–visible and ^2H NMR spectra. Figure 1 shows a series of low-temperature ^2H NMR spectra at various times after treatment of Mn(TPP-d_8)Cl with

(15) Lavallee, D. K. *Bioinorg. Chem.* **1976**, *6*, 219.
(16) Latos-Grazynski, L.; Jezierski, A. *Inorg. Chim. Acta* **1985**, *106*, 13.
(17) Cady, G. H. In *Inorganic Synthesis*; Moeller, T., Ed.; McGraw-Hill: New York, 1957; Vol. V, pp 156–165.
(18) Braun, G. In *Organic Synthesis*; Carothers, W. H., Ed.; Wiley: New York, 1933; Vol. 13, pp 86–89.
(19) Van Geet, A. L. *Anal. Chem.* **1970**, *42*, 679.
(20) Evans, D. F. *J. Chem. Soc.* **1959**, 2003.
(21) Behere, D. V.; Mitra, S. *Inorg. Chem.* **1980**, *19*, 992.
(22) Lagodzinskaya, G. V.; Klimendo, I. Y. *J. Magn. Reson.* **1982**, *49*, 1.
(23) Mellan, I. *Industrial Solvents Handbook*, 2nd ed.; Noyes Data Corp.: Park Ridge, NJ, 1977; p 116.
(24) Perrin, D. D.; Armarego, W. L. F.; Perrin, D. R. *Purification of Laboratory Chemicals*, 2nd ed.; Pergamon: New York, 1980; p 205.

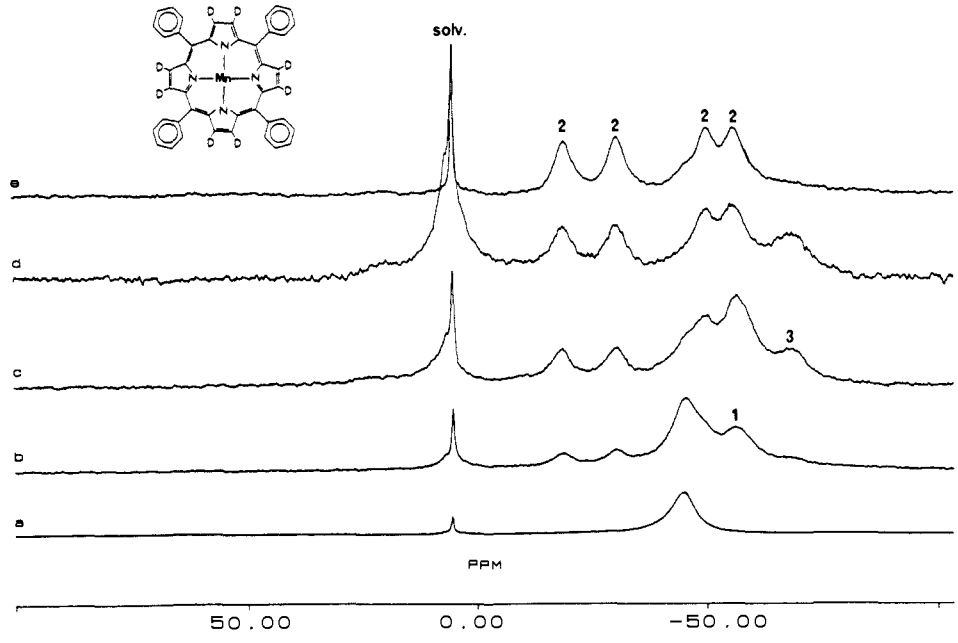

Figure 1. (a) ^2H NMR spectrum of Mn(TPP-d_8)Cl in CH_2Cl_2 at −83 °C. (b) After addition of OCl_2 at −78 °C. (c and d) Spectra representing successive additions of approximately 0.7 mol equiv of OCl_2 at −78 °C. (e) Spectrum of the solution in (d) after 1 day at −78 °C. The intensity in the diamagnetic region is attributed to porphyrin degradation.

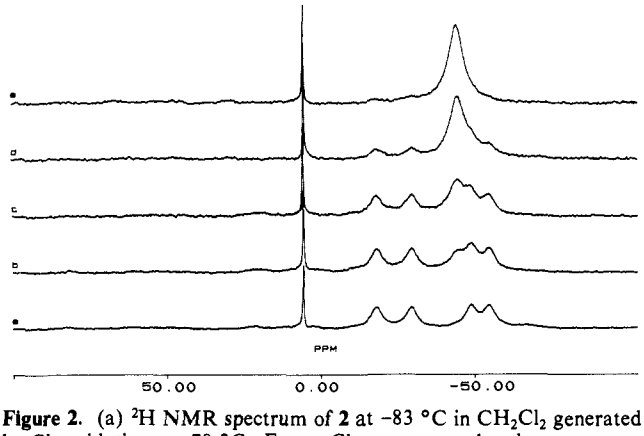

Figure 2. (a) ^2H NMR spectrum of **2** at −83 °C in CH_2Cl_2 generated by Cl_2 oxidation at −78 °C. Excess Cl_2 was removed under pump vacuum at −78 °C and the complex was redissolved in CH_2Cl_2 at −78 °C. (b–e) Spectra representing stepwise addition of 1.0 mol equiv of Bu_4NI in 0.25-equiv aliquots at −78 °C.

OCl_2 at −78 °C. The NMR spectra are presented from +100 to −100 ppm to reflect the absence of a β-pyrrole signal from Mn(TPP-d_8) (55.3 ppm at −83 °C). Over the course of time represented by these spectra, simultaneous increases and decreases in intensities are observed, as what appears to be kinetically favored products (−60 and −66 ppm; **1** and **3**, respectively) ultimately give way to a complex of higher thermodynamic stability. The thermodynamically favored reaction product (**2**) exhibits a four-line ^2H NMR spectrum, with all four lines being of equal intensity. Upon treatment of Mn(TPP-d_8)X (X = Cl^- or OAc^-) with OCl_2 at −160 °C in Freon 22, **1** is observed exclusively via low-temperature ^2H NMR upon careful warming of the sample to −78 °C. This species is slowly (hours) converted to **2** at −78 °C and rapidly (minutes) at −60 °C. The four lines of this spectrum do indeed arise from a single species as demonstrated by the series of spectra in Figure 2. This series of spectra depicts the titration of **2** with iodide ion and shows the intensity of all four lines decreasing in concert with simultaneous growth of the β-pyrrole signal due to Mn(TPP-d_8)X. A similar series of spectra is observed upon stepwise thermal degradation of **2**. The single β-pyrrole deuteron resonance in the NMR spectrum of **1** is indicative of a complex with axial symmetry. Although the high thermal instability of **1** precludes elucidation of its effective magnetic moment, its ESR spectrum, as seen in Figure 3A, with

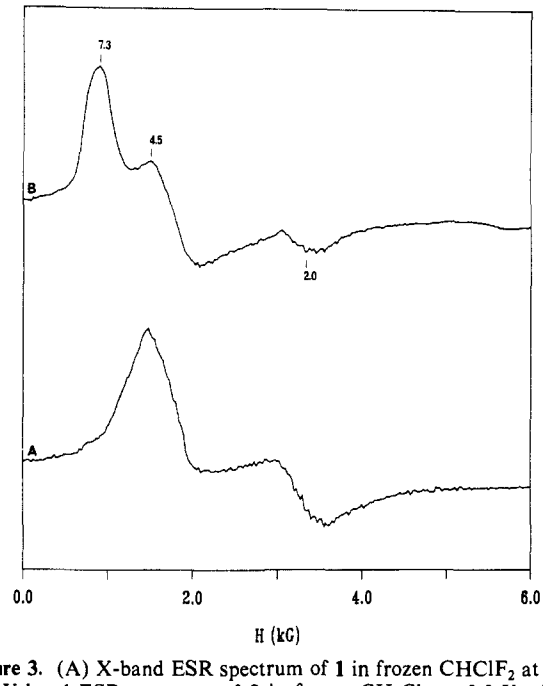

Figure 3. (A) X-band ESR spectrum of **1** in frozen $CHClF_2$ at 5.5 K. (B) X-band ESR spectrum of **2** in frozen CH_2Cl_2 at 5.5 K. Unless otherwise stated, ESR parameters were as stated in the Materials and Experimental Section.

broad resonances at $g = 4$ and a line with a derivative shape at $g = 2$, suggests either a mixture of a high-spin monomeric $S = {}^3/_2$ (porphinato)manganese(IV) complex[25] and a well-relaxed $S = {}^1/_2$ radical or a manganese(IV) porphyrin π-cation radical complex.[26]

Both thermal and photochemical decomposition of OCl_2 result in the production of Cl_2.[27] The presence of Cl_2 in our OCl_2 solutions was verified via iodometric titration.[17] As Cl_2 was always present in our OCl_2 solutions, the possibility of molecular chlorine

(25) Camenzind, M. J.; Hollander, F. J.; Hill, C. L. *Inorg. Chem.* **1983**, *22*, 3776.
(26) Goff, H. M.; Phillippi, M. A.; Boersma, A. D.; Hansen, A. P. In Advances in Chemistry Series 201; American Chemical Society: Washington, DC, 1982; p 357.
(27) Renard, J. J.; Bolker, H. I. *Chem. Rev.* **1976**, *76*, 487.

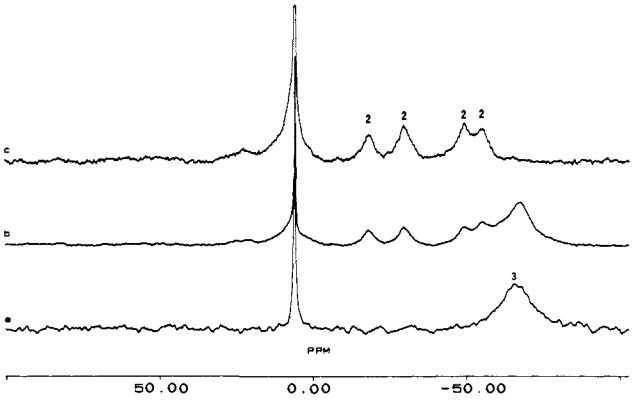

Figure 4. (a) ^2H NMR spectrum of **3** generated by MCPBA oxidation in CH_2Cl_2 at −83 °C. (b) ^2H NMR spectrum of the solution from (a) after treatment with excess Cl_2 at −78 °C and several hours at −78 °C. (c) Low-temperature ^2H NMR spectrum of the solution from (b) after 48 h at −78 °C. Intensity in the diamagnetic region of the spectrum corresponds to degradation products.

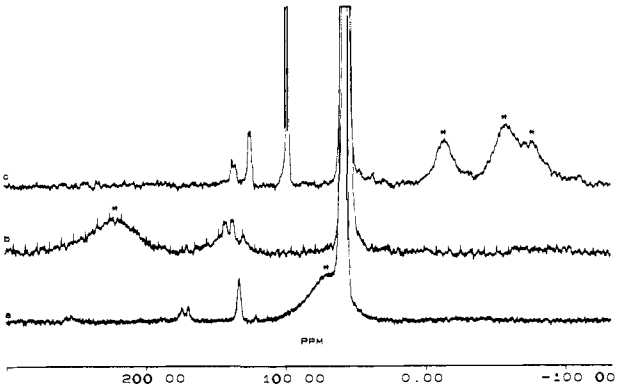

Figure 5. (a) ^{13}C NMR spectrum of Mn(*meso*-[^{13}C]TPP)Cl in CH_2Cl_2 at −60 °C. (b) ^{13}C NMR spectrum of **3** in CH_2Cl_2 at −60 °C generated by MCPBA oxidation at −78 °C. (c) ^{13}C NMR spectrum of **2** in CH_2Cl_2 at −60 °C. Signals rising from porphyrin *meso*-carbon atoms are indicated with an asterisk. The spectra were acquired at −60 °C in order to better resolve the lines in (c). Complexes **2** and **3** were shown to be stable at −60 °C for at least the time required for NMR spectral acquisition.

involvement in this chemistry could not be overlooked. Despite an earlier report that Cl_2 was inefficient as an oxidant for Mn(TPP-d_8)X at room temperature,[28] we found that treatment of these complexes, as well as **1** and **3**, with Cl_2 at −78 °C produces **2** in essentially 100% yield on the basis of ^2H NMR spectroscopy. The presence of varying amounts of water has no effect upon formation of **2**. Likewise, the reaction is insensitive to the presence of oxygen. In fact, **2** forms in spite of the scrupulous exclusion of water and O_2 from the NMR tube reaction. This suggests that chlorine can act independently to oxidize Mn(TPP)X by one or more electrons. Moreover, chlorine or a chlorine byproduct can undergo a bond-forming reaction with **3** at −78 °C to produce **2** as seen in Figure 4. Titration of **2** with iodide ion by using ^2H NMR to monitor the extent of titration revealed one oxidizing equivalent (with respect to the manganese(III) starting material) per mole of **2**. The UV–visible absorption spectrum of **2** contains broad bands centered at 406 and 520 nm. It is worth noting that, in spite of the resemblance of this spectrum to that for a (μ-oxo)manganese(IV) tetraphenylporphyrin dimer, this optical absorption spectrum corresponds to a totally different complex.

The chemical shift multiplicity seen for **2** indicates that it lacks the 4-fold symmetry that is characteristic of most tetraarylporphinato complexes. In order to determine how the 4-fold symmetry of the porphyrin is broken in **2**, its ^{13}C NMR spectrum was recorded. Complex **2** was generated by reaction of Cl_2 with Mn(TPP)Cl in which the *meso*-carbon was enriched to 70% ^{13}C. If **2** were to have a σ_v plane that contained the metal ion and two pyrrole nitrogen atoms, the ^{13}C NMR spectrum would be expected to contain two *meso*-carbon resonances of equal intensity (area). If, on the other hand, the σ_v plane were to contain the metal ion and two *meso*-carbons, the ^{13}C NMR spectrum would be expected to contain three *meso*-carbon signals in a 1:2:1 intensity pattern. Examination of Figure 5 reveals that the latter model is consistent with the spectroscopic results. Note that the *meso*-carbon resonance for **3** is shifted downfield of TMS, whereas those for **2** are upfield shifted. Thus, any contamination from **3** would not interfere with the following interpretation. The ^{13}C NMR spectrum in Figure 5 contains three *meso*-carbon resonances, two of which are overlapping. Cut-and-weigh integration of the overlapping upfield resonances against the single line confirms a respective ratio of 3:1, thus indicating that the overlapping peaks account for three *meso*-carbon atoms and the single peak accounts for the one remaining *meso*-carbon atom.

Previously, we reported that the ^{13}C NMR spectrum of **2** was indicative of a symmetry perturbation in a vertical plane containing the metal ion and two pyrrole nitrogen atoms.[8] However, the earlier ^{13}C spectrum was acquired in $CHClF_2$. The low solubility of the paramagnetic porphyrin complexes in this solvent pushed the sensitivity limits of the NMR instrumentation employed in the experiment. Coupled with the need for extensive base-line correction as a result of severe acoustic probe ringing, it is not inconceivable that the relative intensities of the lines of interest were distorted. Since our earlier report, we have learned that reaction of Mn(TPP)X with molecular chlorine cleanly yields **2** at near dry-ice temperatures. Hence, **2** can now be generated in much higher concentrations as a CH_2Cl_2 solution than was previously possible in Freon 22. Consequently, the meso ^{13}C NMR resonances in the most recent experiments were much more intense than those observed in the initial spectra. We attribute the difference in apparent relative intensities to the increased accuracy with which the intensities could be evaluated in the latest spectra.

Table I.[a] β-Pyrrole Deuteron Isotropic Shift as a Function of Temperature for **2**

$\Delta H_{iso}/H$		
T = −86 °C	$T = \infty$	slope
−18.6	0.6 ± 2.4	−5268 ± 27
−30.5	5.0 ± 2.4	−8295 ± 5
−50.1	4.2 ± 2.4	−11820 ± 21
−56.3	5.4 ± 2.4	−13154 ± 17

[a] Spectra acquired at 55 MHz in CH_2Cl_2 between 177 and 270 K. [b] Slopes and intercepts were obtained from nonweighted linear least-squares fits of the data.

In an effort to compare the chemical shift perturbation observed for **2** with that of a known pyrrole N-perturbed system, the ^2H NMR spectrum of Mn[*N*-CH_3TPP]Cl^+ was acquired at −83 °C. The hyperfine shift pattern for this complex was vastly different from that observed for **2**.[29] The contrast seen in these NMR spectra is considered further evidence that **2** is not a pyrrole-N-perturbed (porphinato)manganese complex.

All four of the signals in the ^2H NMR spectrum of **2** exhibit Curie behavior. The variable-temperature data are compiled in Table I. The complex has an effective magnetic moment of 4.8 ± 0.1 μ_B. This is consistent with an S = 2 spin system that contains manganese formally in its +3 oxidation state. The effective magnetic moment is independent of temperature at and above −92 °C. This temperature-independent magnetic moment is further evidence that the four lines in Figure 2a result from a single species insofar as it indicates a constant and integral number of electronic spins associated with the metal center. Figure 3B presents the ESR spectrum of **2**. This spectrum exhibits broad resonances at g = 7.3, 4.5, and 2.0. This spectrum is discussed at greater length below. Reaction of **2** with cyclohexene results in allylic oxidation and chlorination products with no detectable epoxide formation.

(28) Carnieri, N.; Harriman, A. *J. Chem. Soc., Dalton Trans.* **1982**, 1231.

(29) Yet unpublished work performed in this laboratory.

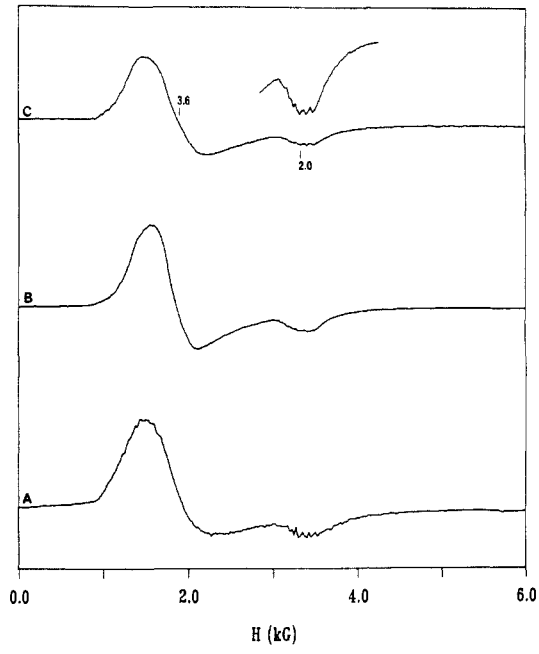

Figure 6. (a) ESR spectrum of **3** generated by MCPBA oxidation of Mn(TPP)OAc at −78 °C in CH_2Cl_2. (B) ESR spectrum of **4** generated via MCPBA oxidation of Mn(TMP)Cl in CH_2Cl_2 at −78 °C. This spectrum corresponds to the ^2H NMR spectrum in Figure 7e. (C) ESR spectrum of **4** generated via OCl_2 oxidation of Mn(TMP)Cl in CH_2Cl_2 at −78 °C.

T_1 measurements at −83 °C for the β-pyrrole deuterons of **2** reveal that all of the deuterons have T_1's between 3 and 4 ms. The experimental uncertainty in these values prohibits the drawing of any conclusions regarding the symmetry of the molecule.

Reactions of MCPBA with Mn(TPP)X and Mn(TMP)Cl. Although **3** cannot be produced exclusively via OCl_2 oxidation, it can be made in significant yields if the oxidation is carried out at or above −78 °C. If OCl_2 is used as the oxidant. **3** gives way to **2**, leaving the four-line spectrum shown in Figure 2a. However, **3** is generated exclusively via MCPBA oxidation at −78 °C. Oxidation of Mn(TPP-d_8)X by 1 or 2 mol equiv of MCPBA at −78 °C is quite slow. The reaction rate is increased considerably by warming the solution to −60 °C (i.e. the reaction goes to completion in minutes rather than hours). In this case Cl_2 must be added after reaction with MCPBA to generate **2** (Figure 4). The analogous complex can be generated by treatment of the very sterically protected Mn(TMP-d_8)Cl with MCPBA at −78 °C. The resulting complex (**4**) also has a β-pyrrole deuteron chemical shift of −66 ppm and an effective spin-only magnetic moment of 3.9 ± 0.1 μ_B, indicative of a monomeric $S = {}^3/_2$, high-spin manganese(IV) complex with little or no spin–orbit coupling. Titration of Mn(TMP-d_8)OAc with MCPBA at −78 °C reveals that 1 mol of MCPBA is required to make 2 mol of **4**. Figure 6 shows the highly anisotropic ESR spectra of **3** and **4** with their broad features at $g = 3.6$ and 2.0 (obtained from the maxima in the integrated spectra). These spectra are consistent with monomeric $S = {}^3/_2$ complexes as reported by Camenzind et al.[25] These data suggest that **4** is an oxo(tetramesitylporphinato)manganese(IV) complex. The second mole of oxygen is postulated to come from residual water in the solvent and from the MCPBA stock.[30] This assignment is also in accordance with FABMS reported by Groves et al.[31]

Figure 7 shows ^2H NMR spectra of **3** and **4** generated by reaction with MCPBA and OCl_2 at low temperature. These spectra reveal the specificity for formation of **3** and **4** via MCPBA oxidation alluded to earlier as well as the lack of specificity observed in the case of Mn(TPP)X oxidation with OCl_2. Figure 7 contains ^2H NMR spectra acquired in CH_2Cl_2 and $CHClF_2$. The chemical shift for Freon 22 is downfield from that for CH_2Cl_2. Consequently, the solvent signals in Figure 7 are offset from one spectrum to the next. Though the porphyrin chemical shifts are very similar from one solvent to the other, the line widths at −83 °C are greater in CH_2Cl_2. This is a correlation time effect resulting from an increase in viscosity of CH_2Cl_2 at the low temperature. This effect is even more dramatic in toluene at such low temperatures. The UV–visible absorption spectrum of **4** contains a single broad band at ϵ_{max} = 416 nm, which is typical of manganese(IV) complexes, whether monomeric or dimeric.

Complex **4** cannot be made to form a TMP analogue of **2**. Furthermore, reaction of cyclohexene with the (tetraphenylporphyrin)manganese complex solutions represented by the spectra in Figure 7 shows high specificity for epoxide formation when MCPBA is used as the source of oxidizing equivalents. Oxidation with OCl_2, however, leads only to trace epoxide formation with most of the products resulting from allylic oxidation and chlorination. Thus, the presence of Cl_2 or a source of Cl_2 causes (either directly or indirectly) **2** to dominate the reaction chemistry of the Mn(TPP)X system.

Meunier et al. have documented that certain pyridine and imidazole derivatives of Mn(TPP-d_8)X greatly enhance its catalytic activity and specificity with regard to olfin epoxidation.[3] In view of our observation that specificity for epoxidation is severely reduced in the presence of **2**, the effect of a pyridine ligand upon its formation and/or its stability is of interest in the understanding of this system. Titration of Mn(TPP-d_8)Cl with 4-methylpyridine at −78 °C reveals the formation of a mono(4-methylpyridyl) (4-Mepy) complex of Mn(TPP-d_8)Cl with a K_d of 30 M at −70 °C. Both the parent and 4-Mepy complexes contain manganese in the +3 oxidation state based upon a temperature-independent effective magnetic moment of 5.1 ± 0.1 μ_B for the solution mixtures over a temperature range from −93 to −22 °C. Treatment of this solution with OCl_2 or Cl_2 at −78 °C does not result in the formation of **2**. Failure of **2** to form was demonstrated by the ^2H NMR spectra of the products of Cl_2 and OCl_2 reaction with Mn(TPP-d_8)(4-Mepy)Cl at −78 °C. In the presence of 4-methylpyridine, Cl_2 and OCl_2 give axially symmetry Mn(TPP-d_8)X oxidation products in varying yields. These high-valent complexes have ESR spectra characteristic of a monomeric $S = {}^3/_2$ spin system.[25] Treatment of Mn(TPP-d_8)(4-Mepy)Cl with MCPBA at −78 °C results in a mixture of species whose ^2H NMR spectrum is difficult to interpret. This is most likely due to side reactions of MCPBA with 4-methylpyridine. For example, production of 4-methylpyridine *N*-oxide could lead to formation of as yet unobserved complexes.

Mn(TPP)X and Mn(TMP)Cl Oxidation in the Presence of OH^-. It is noteworthy that, despite repeated attempts to stabilize manganese(V) by low-temperature oxidation of Mn(TPP)X and Mn(TMP)Cl in the presence of hydroxide ion, we were unable to observe manganese(V) spectroscopically.[31] Parts A and B of Figure 8 contain the ESR spectra of the MCPBA oxidation products of Mn(TPP)OAc and Mn(TMP)Cl in the presence of OH^-. Both spectra are indicative of monomeric $S = {}^3/_2$ (porphinato)manganese(IV) complexes. Integration of these spectra vs Cr(TPP)Cl (used as an $S = {}^3/_2$ standard) revealed that the ESR intensity represented by the spectra in parts A and B of Figure 8 accounted for all of the manganese (>90%) in the starting material. This was the case whether oxidation was carried out at −78 or −160 °C.

We have investigated the speciation of high-valent (tetraarylporphinato)manganese complexes in the presence of hydroxide ion. Treatment of **2** with hydroxide ion (as a 1M Bu_4NOH solution in CH_3OH) at −78 °C results in an $S = {}^3/_2$ (ESR) species that has a β-pyrrole deuteron chemical shift of −32 ppm (−83 °C) in the ^2H NMR spectrum. A species with a β-pyrrole shift of −37 ppm at −83 °C (**5**) can be generated by treatment of Mn(TPP-d_8)X with OCl_2 in the presence of 2 mol equiv of hydroxide ion at −78 °C. This complex is stable for hours in solution at room temperature. The formation of this species was verified and monitored via low-temperature NMR. An analogous Mn(TMP-d_8) complex (**6**) can be generated under the same conditions

(30) Williamson, M. M.; Hill, C. L. *Inorg. Chem.* **1987**, *26*, 4155.
(31) Groves, J. T.; Stern, M. K. *J. Am. Chem. Soc.* **1987**, *109*, 3812.

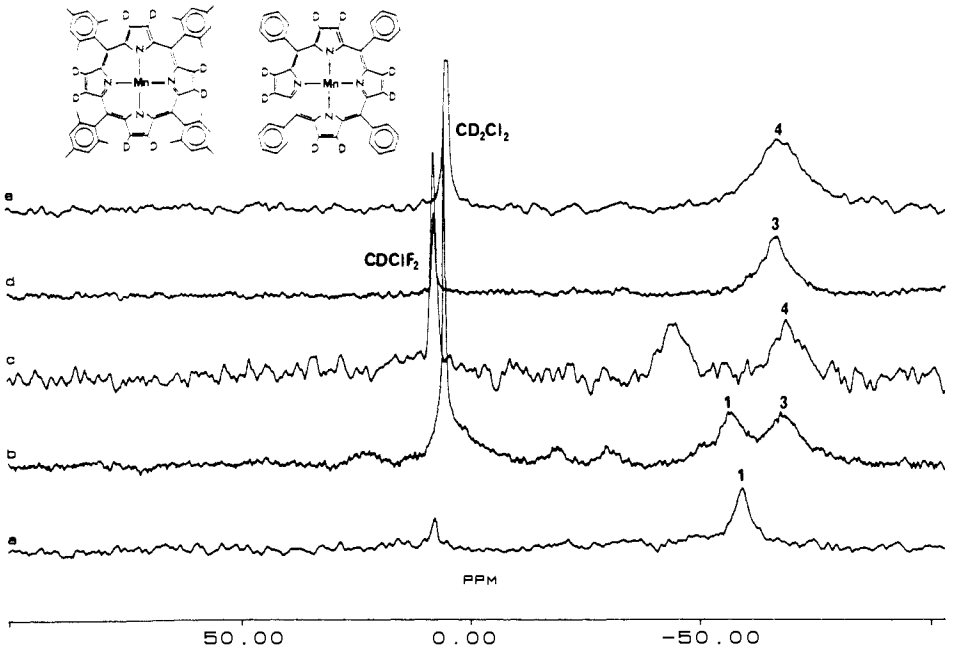

Figure 7. (a) ^2H NMR spectrum of **1** generated by OCl_2 oxidation of Mn(TPP-d_8)OAc in $CHClF_2$ at −160 °C. Spectra were acquired at −83 °C. (b) ^2H NMR spectrum of a mixture of **1–3** generated via OCl_2 oxidation of Mn(TPP-d_8)Cl in CH_2Cl_2 at −78 °C. (c) ^2H NMR spectrum of **4** generated by OCl_2 oxidation of Mn(TMP-d_8)Cl in $CHClF_2$ at −78 °C. The peak at −49 ppm is unreacted starting material. (d) ^2H NMR spectrum of **3** generated by MCPBA oxidation of Mn(TPP-d_8)OAc at −78 °C in $CHClF_2$. (e) ^2H NMR spectrum of **4** generated via MCPBA oxidation of Mn(TMP-d_8)Cl at −78 °C in CH_2Cl_2.

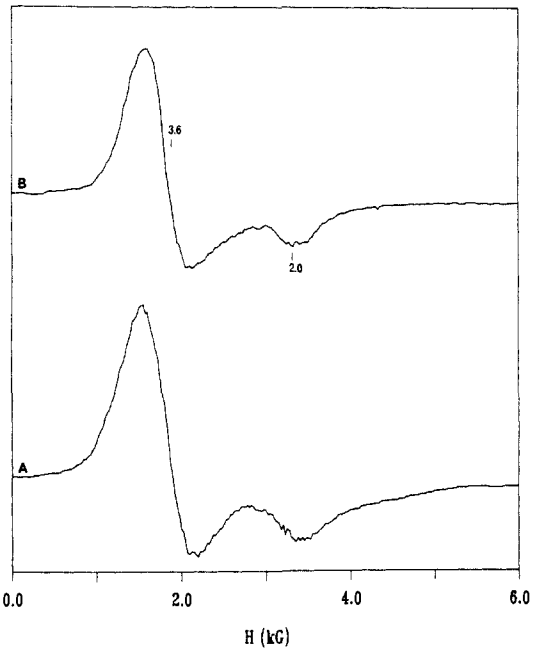

Figure 8. (A) ESR spectrum of **5** and precursor species generated by MCPBA oxidation of Mn(TPP)OAc in the presence of 2.0 mol equiv of Bu_4OH in CH_2Cl_2 at −78 °C. (B) ESR spectrum of **6** and precursor species generated in the same manner as **5**.

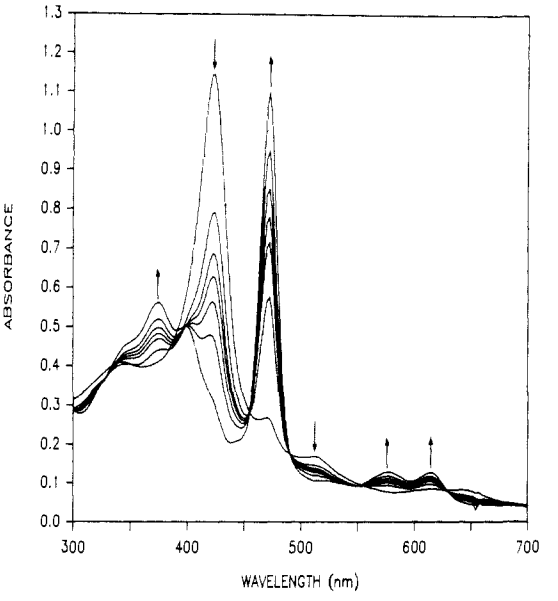

Figure 9. Series of UV–visible absorption spectra illustrating the room-temperature reduction of **5** (1.3×10^{-5} M) by cyclohexene (0.5 M) in CH_2Cl_2. Bands at 422 and 520 nm correspond to **5**. The spectra correspond to 0, 0.2, 1.2, 5.2, 10.2, 20.2, and 120.2 min after addition of cyclohexene to the solution of **5**. Complex **6** exhibits analogous behavior under these conditions.

using OCl_2 or MCPBA as the oxidant and exhibits a β-pyrrole shift of −40 ppm in the ^2H NMR spectrum. In the generation of **5** and **6**, the reactions proceed through mixtures containing a second major species with β-pyrrole shifts at −52.5 and −53.5 ppm, respectively. The detailed nature of these intermediate species remains somewhat ambiguous. However, the ESR spectra of **5** and **6** in their respective "precursor mixtures" shed some light on the circumstances of these reactions. The spectra in parts A and B of Figure 8 correspond to the respective precursor mixtures for **5** and **6**. These spectra are all indicative of monomeric $S = {}^3/_2$ (porphinato)manganese(IV) complexes. As the spectra in parts A and B of Figure 8 account for essentially all of the manganese in the samples, **5** and **6** and their respective precursor species are all concluded to be monomeric (porphinato)manganese(IV) complexes. These complexes differ from the starting hydroxide complex, which has a β-pyrrole shift of −40 ppm in the ^2H NMR spectrum at −83 °C and a temperature-independent effective magnetic moment of 4.9 ± 0.1 μ_B at the temperatures of these reactions.

Complexes **5** and **6** react with cyclohexene to regenerate Mn(TPP)X as demonstrated via monitoring of the solution's electronic absorption spectrum. Figure 9 illustrates the changes in the UV–visible spectrum at room temperature as a function of time following the addition of cyclohexene. The time period represented by Figure 9 is 2 h. Identical treatment of Mn(TMP)Cl results in spectra that are virtually superimposable with those in Figure

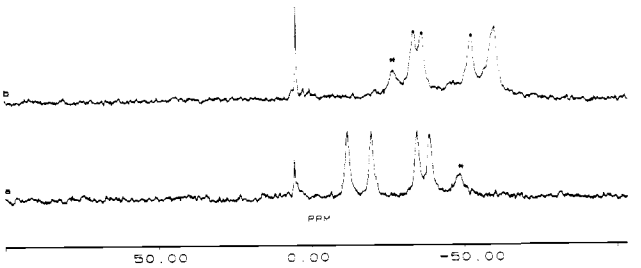

Figure 10. (a) ^2H NMR spectrum of complex **2** in CH_2Cl_2 at −22 °C. The asterisk indicates the presence of a small amount of **3**, which begins to form at temperatures above −40 °C. (b) ^2H NMR spectrum of complex **2a** in CH_2Cl_2 saturated with Pr_4NClO_4 acquired at −22 °C. The asterisk indicates a small amount of unoxidized Mn(TPP-d_8)Cl.

9. Assignment of the initial spectrum in Figure 9 to a manganese(IV) complex is in contrast to a previous report identifying the Mn(TPP) analogue (**5**) as manganese(V).[32]

Electrochemistry of Mn(TPP)X and Mn(TMP)Cl. Complex **3** and an analogue of **2** are also attainable via electrochemical oxidation of Mn(TPP-d_8)Cl. Cyclic voltammetric evaluation of a CH_2Cl_2 solution containing Mn(TPP-d_8)Cl at room temperature or at approximately −60 °C reveals two oxidation waves, one at 1.18 V (all potentials are reported vs SCE) and the second at 1.58 V. Both waves represent quasi-reversible electrode processes. The initial CV scan direction was positive in all cases. In all room-temperature scans where the working electrode potential was raised above 1.4 V, the subsequent cathodic scan produced a reduction wave at 0.6 V that had no oxidative counterpart. When the scan is paused at the potential of the second oxidation wave, the current amplitude of this irreversible wave is significantly increased. Thus, the species that gives rise to this wave results from a chemical reaction of the second oxidation product. This irreversible reduction wave was not observed at low temperature.

Bulk electrolysis at ambient temperature was carried out with the anode held at the potential of the first oxidation wave. Examination of the electrolyzed solution by cyclic voltammetry showed a large increase in the relative current amplitude of the wave at 0.6 V. Furthermore, the wave at 0.6 V was present even if the working electrode potential was not raised to that of the second oxidation wave.

Examination of the low-temperature electrolysis products by low-temperature ^2H NMR and ESR revealed that **3** is formed. Whereas CV analysis of a solution electrolyzed at room temperature and at the potential of the first oxidation wave revealed the presence of a relatively large amount of the complex corresponding to the reduction wave at 0.6 V, a CV scan run after low-temperature bulk oxidation showed no change in the features, i.e. no dramatic increase in current amplitude of the wave at 0.6 V. The species that gives rise to the 0.6-V reduction wave (**2a**) exhibits NMR and ESR spectral features analogous to those of **2**, but its thermal stability is notably higher. Figures 10, 11A, and 11B show the NMR and ESR spectra of **2** and **2a** at equivalent temperatures for comparison. Although the NMR line widths and isotropic shifts of the β-pyrrole deuterons are different in the spectra of **2** and **2a**, the multiplicity and relative intensities of the NMR lines are analogous. The ESR spectrum of **2a** has a notable derivative signal at $g = 2$ that is in contrast to the spectrum of **2**. The $g = 2$ feature is due to the presence of some manganese(III) porphyrin π-cation radical. This species gives rise to a broad β-pyrrole deuterium line at −39 ppm in the room-temperature NMR spectrum and was observed for these samples. Formation of the manganese(III) porphyrin π-cation radical is greatly attenuated in the presence of a 10-fold excess of chloride ion or a 2-fold excess of hydroxide ion (on a molar basis). Thus, such excess of chloride or hydroxide ion favor metal-centered oxidation as opposed to porphyrin ligand-centered oxidation.

(32) van der Made, A. W.; Drenth, W.; Nolte, R. J. M. *Recl. J. Neth. Chem. Soc.* **1987**, *106*, 1-28.

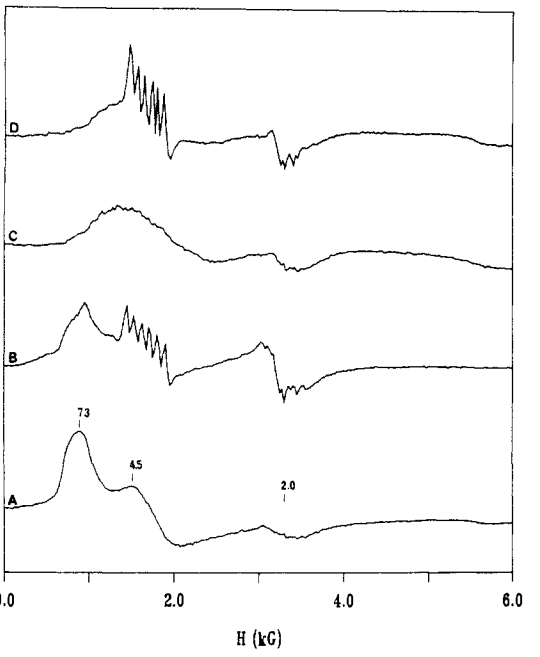

Figure 11. (A) ESR spectrum of **2** generated via Cl_2 oxidation of Mn(TPP)Cl at −78 °C in CH_2Cl_2. (B) ESR spectrum of **2a** in CH_2Cl_2 that was saturated with Pr_4NClO_4 at room temperature. The derivative-shaped signal at $g = 2$ corresponds to some (tetraphenylporphinato)manganese(III) π-cation radical. (C) ESR spectrum of **7a** in CH_2Cl_2 that was saturated with Pr_4NClO_4 at room temperature. (D) ESR spectrum of **7b**; conditions as in (C). Spectra acquired in frozen CH_2Cl_2.

After electrolysis at the potential of the second oxidation wave at 1.58 V (no added Cl^- or OH^-), the manganese(III) porphyrin π-cation radical is no longer observed in the NMR spectrum. It is superseded by a minor species with a β-pyrrole chemical shift of −51 ppm at 25 °C. Characterization of this species was not pursued. The four NMR lines of the asymmetric complex are still present after electrolysis at 1.58 V. After the solutions stand for hours or upon manipulation of the solutions to remove the supporting electrolyte, these species revert to the π-cation radical with a β-pyrrole NMR signal at −39 ppm at 25 °C. This assignment is further supported by the electronic spectrum, which corresponds with that reported for the manganese(III) porphyrin π-cation radical.[26] As the electrochemically produced oxidation product described in a previous report from this laboratory was freed from the supporting electrolyte required for its production, the only product observed spectroscopically was the manganese(III) porphyrin π-cation radical.[26] The inability to maintain the integrity of **2a** through removal of the supporting electrolyte precluded reliable determination of an effective magnetic moment for this complex.

Examination of Mn(TMP)Cl via room-temperature CV showed no irreversible reduction wave near 0.6 V. No asymmetric species were observed upon bulk electrolysis of Mn(TMP)Cl at the first or second oxidation potentials. Two "first" oxidation waves were observed in the CV scans of Mn(TMP)Cl. The lowest potential wave (1.08 V) was only observed in the first scan of a fresh solution. Subsequent scans revealed a wave anodically shifted to 1.18 V. Room-temperature electrolysis at 1.08 V resulted in species giving a single-line ^2H NMR spectrum at room temperature (**7a**). Electrolysis at 1.18 V produced a solution that had the same ^2H NMR spectrum but a different ESR spectrum from that exhibited by **7a** (**7b**). The room-temperature β-pyrrole chemical shift for these complexes was observed at −20 ppm. The ESR spectra are indicative of $S = {}^3/_2$ (porphinato)manganese(IV) complexes (see parts C and D of Figure 11). The UV–visible absorption spectra of **7a** and **7b** contain a broad absorbance at $\epsilon_{max} = 384$ nm and a less intense band centered around 615 nm at room temperature. Bulk electrolysis of Mn(TMP)Cl at its second oxidation potential (ambient temperature) resulted in degradation of the porphyrin macrocycle.

Table II.[a] Physical Properties of (Porphinato)manganese Complexes

complex	starting material	oxidizing agent	β-pyrrole shift, ppm	spin state (S) via ESR	μ_{eff}, μ_B	opt abs max, nm
1	Mn(TPP)X	OCl_2	−60[b]	$^3/_2$, $^1/_2$		
2	Mn(TPP)X	OCl_2, Cl_2	−19, −30, −50, −56	$^3/_2$, $^5/_2$	4.9 ± 0.1	406, 520
2a	Mn(TPP)X	elect	−33, −36, −52, −59[c]	$^3/_2$, $^5/_2$, $^1/_2$[d]		320, >820[e]
3	Mn(TPP)X	MCPBA	−66	$^3/_2$		
4	Mn(TMP)Cl	MCPBA	−66	$^3/_2$	3.9 ± 0.1	416
5	Mn(TPP)X	OCl_2	−37	$^3/_2$		422, 520
6	Mn(TMP)Cl	OCl_2	−40	$^3/_2$		422, 520
7a	Mn(TMP)Cl	elect	−20	$^3/_2$		384, 615
7b	Mn(TMP)Cl	elect	−20	$^3/_2$		384, 615

[a] Unless otherwise specified, temperature was −83 °C for NMR experiments and 5.5 K for ESR experiments, and solvent was CH_2Cl_2. [b] Generated in $CHClF_2$ at −160 °C. [c] Spectrum acquired at −22 °C. [d] $S = ^1/_2$ component of the spectrum arises from residual manganese(III) porphyrin π-cation radical. [e] The tail of a band is apparent at the low-energy edge of the spectrum.

Discussion

The flow charts in Figure 12 are included as a general aid to discussion of manganese porphyrin reaction chemistry. The complexes involved in the pathways illustrated by Figure 12 are listed in Table II along with their respectively physical constants and spectral features.

Formation of the Low-Symmetry Products. On the basis of symmetry and spin-state information obtained via spectroscopic methods as described above, we suggest that **2** and **2a** are manganese(III) isoporphyrins of similar structure but with different symmetry-perturbing meso substituents. The following discussion addresses the details of this hypothesis.

The prerequisite for isoporphyrin formation with common nucleophiles is a doubly oxidized metalloporphyrin ring.[33] The formation of an isoporphyrin as a result of room-temperature electrolysis at the potential of the first oxidation wave in the CV scan could be the manifestation of a small steady-state concentration of a doubly oxidized complex. The first oxidation wave is separated from its reduction counterpart by approximately 80 mV, which indicates that, although the electrode process is not totally reversible, these waves represent a one-electron process. Thus, there must be a nonelectrode pathway to formation of a doubly oxidized complex from the single oxidized species, namely disproportionation. As the presence of coordinating ligands such as Cl^- or OH^- in excess favors metal-centered oxidation and precludes formation of **2a** upon electrolysis at the potential of the first oxidation wave, the production of a manganese(III) porphyrin π-cation radical is concluded to be necessary to the production of **2a**.

The electrolytic oxidation product **2a** also fails to form upon low-temperature (approximately −60 °C) oxidation of Mn(TPP)X at the first oxidation potential. Examination of Mn(TPP)X solutions by CV at low temperature shows no isoporphyrin formation (no reduction wave at 0.6 V. Additionally, low-temperature electrolysis of Mn(TPP)X at the potential of the first oxidation wave in the cyclic voltammogram resulted in the production of **3**. This was verified by ^2H NMR and ESR spectroscopies. This means that either the chemical reaction that leads to **2a** is very slow at these temperatures or **3** does not disproportionate to give a doubly oxidized (porphinato)manganese complex. Hence, insofar as a doubly oxidized porphyrin ligand is necessary for the formation of a metalloisoporphyrin, low temperatures preclude formation of **2a**.

Tetramesitylporphyrin is generally more robust than the less substituted tetraarylporphyrin analogues with respect to chemical attack of the porphyrin macrocycle. Thus, the failure to form the **2a** analogue of Mn(TMP)Cl upon bulk oxidation at the first oxidation potential can be taken as further evidence for assignment of **2a** as an isoporphyrin. Indeed, upon bulk electrolysis of Mn(TMP-d_8)Cl at its first oxidation potential, there is no indication that an analogue of **2a** has formed. This is evidenced by the absence of a four-line β-pyrrole ^2H NMR spectrum. Moreover, the ESR spectrum of the electrolyzed solution revealed clean

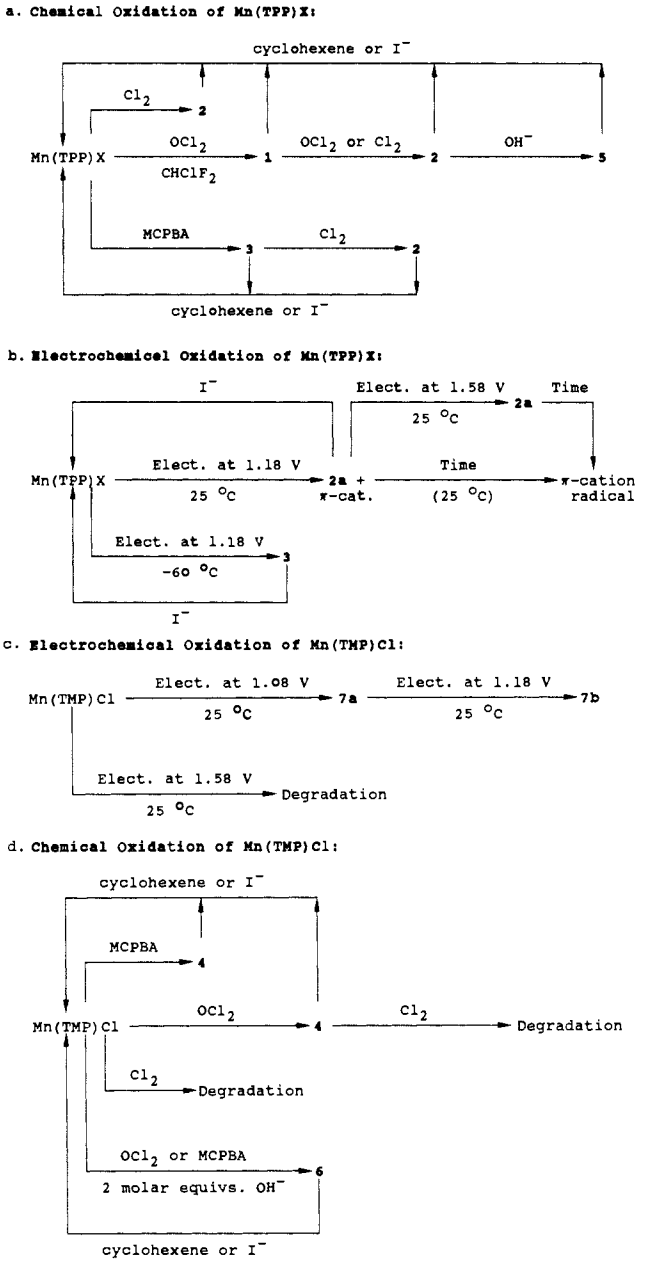

Figure 12. Flow charts describing the fate of (porphinato)manganese complexes upon various treatments and manipulations.

production of a monomeric (porphinato)manganese(IV) complex. It is interesting to note that a CV scan of virgin 0.1 mM Mn(TMP)Cl in CH_2Cl_2 reveals the first oxidation wave at 1.08 V. However, a subsequent scan (i.e. no time between scans) reveals that the potential of the first oxidation wave shifts to 1.18 V. Electrolysis at 1.08 V results in a complex (**7a**) that exhibits the

(33) Felton, R. H. In *The Porphyrins*; Dolphin, D., Ed.; Academic: New York, 1978; Vol. V, pp 81-88.

ESR spectrum shown in Figure 11C, whereas electrolysis at 1.18 V produced a complex (**7b**) that afforded the spectrum in Figure 11D. The lack of an oxygen atom donor (such as MCPBA, OCl_2, or iodosylbenzene) drives manganese(IV) to hexacoordination in order to balance the charge of the metal center. The observation of two first oxidation potentials is consistent with formation of a six-coordinate manganese(IV) complex (during the first scan) that does not undergo significant ligand dissociation on the time scale of the CV experiment. The subsequent anodic potential scan results in a wave at the first oxidation potential of the six-coordinate manganese(III) complex (1.18 V) rather than at the potential of the five-coordinate starting material. Thus, generation of ^{55}Mn hyperfine structure in the low-field component of the ESR spectrum shown in Figure 11D is suggestive of six-coordination at the manganese(IV) center with oxygen-bound ligands in both axial positions.[25]

The chemical generation of **2** can be discussed in the context of metal-centered versus ligand-centered oxidation. The fact that formation of **2** does not require water, hydroxide ion, or molecular oxygen implies that the production of **2** is driven by Cl_2 or a byproduct thereof. It is reasonable to suggest that the potent oxidizing ability of Cl_2 generates a steady-state concentration of a singly oxidized (porphinato)manganese(III) complex at temperatures near that of dry ice. Whether the oxidation is primarily metal-centered or ligand-centered, an equilibrium between manganese(IV) and manganese(III) porphyrin π-cation radical can exist.[37] Thus, in the presence of Cl_2, some π-cation radical complex may be generated. As molecular chlorine and chlorine monoxide are viable sources of chlorine atoms,[27] the feasibility of a radical coupling reaction between the π-cation radical complex and chlorine atoms is clear.[33] The result would be singly charged, five-coordinate or a neutral, six-coordinate manganese(III) isoporphyrin complex. Although the manganese ion in **2** is in its +3 oxidation state (magnetic susceptibility), the *meso*-chlorine is formally chlorine(0). Thus, **2** contains available oxidizing equivalents, as demonstrated by its reactivity toward cyclohexene and iodide ion.

The lack of any neutral, odd-electron species renders such a pathway to isoporphyrin formation unavailable in the electrochemical oxidation of Mn(TPP)X. The most likely nucleophiles to be involved in electrochemical generation of isoporphyrins are water and hydroxide ion. Thus, the increased stability of **2a** over **2** results from a lower reduction potential of the modified porphyrin ring in **2a**. The observation that **2a** is converted to the π-cation radical upon standing or handling indicates that formation of the manganese(III) isoporphyrin is reversible, regardless of the nature of the porphyrin-perturbing nucleophile. The tendency for reduction of metalloisoporphyrins has been described.[33]

Despite its effective magnetic moment of 4.9 ± 0.1 μ_B the ESR spectrum of **2** (Figure 3B) is inconsistent with a monomeric $S = 2$ manganese(III) complex. The ESR intensity in spectra of 2 has not been carefully quantitated. However, comparison with the intensity observed in ESR spectra of manganese(IV) at similar concentrations reveals that **2** does not represent a minor species that goes undetected in the NMR experiments. The spectrum in Figure 3B appears as a superposition of an $S = {}^5/_2$ spectrum and an $S = {}^3/_2$ spectrum. Furthermore, there is an observable and reversible color change from brown to green upon freezing the solution. Inasmuch as asymmetric porphyrin ligands are known to stabilize the +2 oxidation states of manganese[15] and iron[34] and in view of the color change to green upon freezing, it is possible that **2** autoreduces upon freezing to afford an asymmetric manganese(II) complex whose ESR spectrum is perturbed to give a low-field doublet. As a means of testing this possibility, the ESR spectrum of Mn[*N*-CH_3TPP]Cl was recorded. The resulting spectrum is shown in Figure 13 along with that of **2** for the sake of comparison. Figure 13B illustrates that, even when the 4-fold porphyrin symmetry is broken at a pyrrole nitrogen atom, the ESR spectrum of the $S = {}^5/_2$ complex does not exhibit

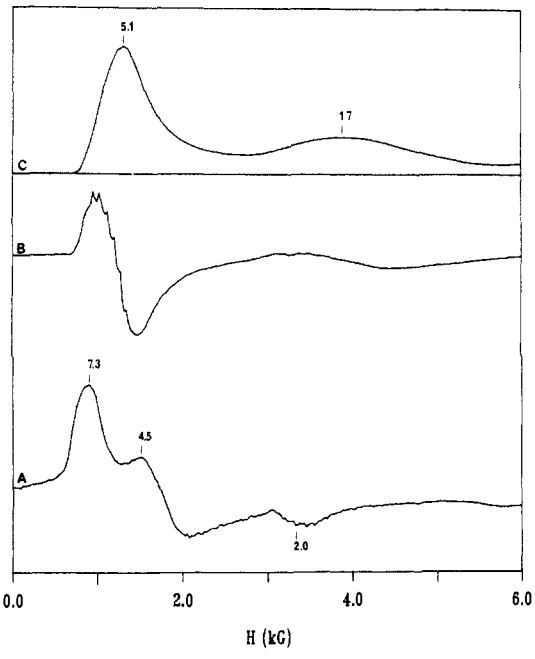

Figure 13. (A) ESR spectrum of **2** in frozen CH_2Cl_2 at 5.5 K. (B) Derivative ESR spectrum of Mn[*N*-CH_3TPP]Cl. (C) Adiabatic rapid passage ESR spectrum of Mn[*N*-CH_3TPP]Cl acquired to visualize the broad resonance centered at 3.8 kG. Spectra B and C acquired in CH_2Cl_2/toluene (1:1 (v/v)) at 5.5 K.

observable splitting of the low-field signal. Hence, the ESR spectrum of **2** cannot be explained strictly in terms of an axially asymmetric $S = {}^5/_2$ manganese(II) complex. These observations suggest disproportionation of **2** upon freezing to give high-spin manganese(II) and high-spin manganese(IV). Hence, we conclude that the ESR spectrum of **2** represents an equilibrium mixture of $S = {}^5/_2$ and $S = {}^3/_2$ (tetraphenylporphinato)manganese complexes that results from disproportionation of **2** upon freezing of the solution.

Although we have demonstrated that **2** can be precipitated and collected by filtration or centrifugation at −78 °C with minimal decomposition, extensive efforts to grow and mount diffraction quality crystals at −78 °C were unsuccessful.

Neither **2** nor **2a** appears to exhibit what is generally considered to be a typical metalloisoporphyrin electronic spectrum. We do not observe any bands in the low-energy region of the visible spectrum. Nevertheless, as manganese isoporphyrins have not been previously characterized, we cannot discount the possibility that these bands are beyond the range of our spectrophotometer (820 nm).[35] In fact, a UV–visible absorption spectrum of **2a** exhibits the "tail" of a band centered at a wavelength >820 nm (Table II).

The fact that **2** forms in the absence of an oxygen source and that it can act as an oxidizing agent suggests that it may be responsible for oxidation pathways that compete with oxygen-transfer reactions. Indeed, it explains the oxidative chlorination observed upon treatment of **2** with cyclohexene. While this tendency of (porphinato)manganese(III) complexes is generally considered problematic in terms in catalytic oxygen-transfer specificity, it has intriguing implications in terms of tailoring reagents for the oxidation and/or oxidative addition to organic substrates.

(Porphinato)manganese(IV) Complexes. Despite the aptitude of Mn(TPP)X for formation of the chlorinating complex discussed above, it is also well-known for its expediency in the facilitation of oxygen-transfer reactions in the presence of chlorine(I) reagents. The remainder of this discussion is thus devoted to the (porphinato)manganese species responsible for this oxygen-transfer chemistry.

(34) Anderson, O. P.; Kopelove, A. B.; Lavalle, D. K. *Inorg. Chem.* **1980**, *19*, 2101.

(35) Gold, A.; Ivey, W.; Tony, G. E.; Sangaiah, R. *Inorg. Chem.* **1984**, *23*, 2932.

There are several redox couples that can be envisioned as being responsible for the two-electron transfer and oxygen transfer from a high-valent manganese complex to an organic substrate. One such couple would involve the manganese analogue of compound I of the peroxidases and cytochrome P450, namely that of manganese(IV) π-cation radical/manganese(III). Such a complex would be a two-electron oxidant with manganese(III) as the "resting state" of the catalyst. Thus, it is conceivable that this complex would be capable of oxo-transfer chemistry. The possibility exists that **1** is an oxo(porphinato)manganese(IV) radical cation species, and its potent reactivity certainly makes it a candidate for a major role in the reaction chemistry of Mn(TPP)X and chlorine(I) compounds. The ESR and NMR data presented above indicate that there is no significant amount of radical present in solutions of **2**, **3**, or **4**. The characteristic broad, intense, $g = 2$ signal is absent from the ESR spectra, and the *meso*-carbon hyperfine NMR shifts for **2** and **3** are much too small to support a π-cation radical assignment. Furthermore, the large alternating positive and negative hyperfine NMR shifts that are characteristic of the phenyl proton or deuteron resonances in TPP^{2-} π-cation radical complexes of iron are not observed for **2** or **3**.[36] This phemonenon is diagnostic for the presence of π-cation radical complexes; however, small shifts are themselves ambiguous. This was demonstrated by electrochemical generation of manganese(III) porphyrin π-cation radical starting with Mn(TPP-d_{20})Cl.[26] The ^2H NMR spectrum revealed no large isotropic shifts of the phenyl signals.

The second possible couple is manganese(V)/manganese(III). Although we cannot completely discount the involvement of manganese(V) in this chemistry, we can offer no spectroscopic evidence for such involvement. Depending upon its spin state, manganese(V) is either an $S = 1$ or an $S = 0$ ion. In either case, a manganese(V) complex is expected to be ESR silent. Thus, the observation of a clean $S = {}^3/_2$ manganese(IV) ESR spectrum is not evidence against the presence of manganese(V), and its presence cannot be discounted on the basis of our inability to observe it spectroscopically. However, we can account for all of the initial manganese(III) (>90%) as manganese(IV) in the ESR spectra of our high-valent complexes generated by low-temperature OCl_2 or MCPBA oxidation. Hence, we conclude that if manganese(V) is present, it exists in a relatively low steady-state concentration. The stoichiometry of (porphinato)manganese(III) oxidation by MCPBA as determined via our NMR titration puts transient existence of manganese(V) (or manganese(IV) porphyrin π-cation radical) within the realm of possibility. Another conceivable pathway to generation of manganese(V) lies in the disproportionation of a singly oxidized manganese(III) complex.

The third possible redox couple is manganese(IV)/manganese(II) with simultaneous oxo transfer to the reducing substrate. The resultant (porphinato)manganese(II) complex would either be ultimately oxidized to manganese(III) by atmospheric oxygen or to manganese(IV) by excess oxidant present in the catalytic system. We have reacted **3** with cyclohexene under scrupulously anaerobic conditions in an effort to see whether manganese(II) is indeed generated through oxygen atom transfer to cyclohexene. We were only able to observe Mn(TPP-d_8)X after the reaction. Thus, either manganese(II) was not produced or it reacted rapidly with manganese(IV) to produce manganese(III).

Complexes **1**, **3**, and **5** are all assigned as (porphinato)manganese(IV) species on the basis of ESR spectra and/or magnetic susceptibility measurements. Each however, exhibits an NMR spectrum unique from the others. Whereas the assignment of **1** as a manganese(IV) porphyrin π-cation radical defines a specific electronic spin-state assignment, the formulation in terms of axial ligation is less than definitive. As several potential coordinating ligands are present in these solutions (Cl^-, OH^-, OCl^-, HOCl, OCl_2, "O^{2-}"), the possible permutations of axial ligation are numerous, and our data do not support a particular formulation for **1**. The increase in thermal stability of **3** over **1** is consistent with a lower valent complex, and the oxygen-transfer efficiency of **3** (with regard to cyclohexene epoxidation) lends support to the assignment of **3** (and **4**) as an oxo(porphinato)manganese(IV) complex.

Role of Pyridine Derivatives. The presence of excess 4-methylpyridine quenches the formation of **2**. The reasons for this behavior are likely 2-fold. Ligand field has been demonstrated to exert a strong influence upon the site of metalloporphyrin oxidation, with weaker ligand fields favoring π-cation radical formation.[37] This is further supported in the present case by the lack of electrochemical manganese porphyrin π-cation radical formation in the presence of excess chloride or hydroxide ion. It has been established that the conversion of manganese(IV) to manganese(III) π-cation radical is mediated by ligand exchange. Thus, the presence of the latter, at least in small concentrations, is inevitable in solutions that contain (porphinato)manganese(IV) complexes.[37] In the presence of a chlorine atom source, the π-cation radical may undergo a chlorination reaction to give an isoporphyrin (**2**) that exhibits the ^2H NMR spectrum in Figure 1c. The coordination of 4-methylpyridine to Mn(TPP-d_8)X or **3** represents an increase in the ligand field experienced by the manganese ion. This stronger ligand field serves to favor metal ion oxidation as opposed to oxidation of the porphyrin macrocycle. On this basis, the general pathway to isoporphyrin formation is shut down in the presence of 4-methylpyridine and **2** cannot form. Small amounts of (porphinato)manganese(IV) typically form under these conditions, presumably due to water present as an impurity in the reaction mixture. While the mixture at hand precluded measurement of an accurate effective magnetic moment for this complex, the ESR spectrum contains broad resonances at $g = 4$ and 2. We, therefore, submit that the low-yield oxidation product of Mn(TPP-d_8)(4-Mepy)Cl with Cl_2 is an oxo(tetraphenylporphinato)manganese(IV) complex. The ability of 4-methylpyridine to quench the formation of **2** may be further promoted by chlorine atom complexation by the pyridine derivative. This phenomenon was recently elaborated upon in the context of three-electron bond formation and its effect upon chlorination specificity by Cl_2.[38] This "tying up" of chlorine atoms may significantly retard their reaction with the porphyrin π-cation radical, thus reducing the efficiency with which the porphyrin ligand is chlorinated.

Role of Hydroxide Ion. As pointed out earlier, treatment of Mn(TPP)X or Mn(TMP)Cl with 2 mol equiv of hydroxide results in a complex with a β-pyrrole chemical shift of approximately −40 ppm at −83 °C. Formation of this complex can be monitored via ^2H NMR. Titration of Mn(TPP-d_8)X with OH^- results in a downfield shift of the β-pyrrole deuterium signal until 2 equiv of hydroxide ion have been added. Treatment of this hydroxide complex with an oxo-transfer agent (OCl_2 or MCPBA) at low temperature results in **5** (or **6** for the case of Mn(TMP)Cl), which is stable on the order of hours in solution at room temperature. Addition of a reducing substrate, however, elicits regeneration of the starting material (Figure 9). We suggest that this stabilization is the manifestation of an acid/base equilibrium between bis(hydroxyporphinato)manganese(IV) and the oxo(hydroxyporphinato)manganate(IV) ion. The added stability of (tetraarylporphinato)manganese(IV) species in the presence of hydroxide ion may have significant implications regarding the understanding of the catalytic hypochlorite oxidation system. It follows that an increase in epoxidation rate is the manifestation of a more reactive catalytic intermediate. A decrease in the basicity of the aqueous phase in the catalytic hypochlorite system has the effect of raising its epoxidation efficiency.[4] This is consistent with our observation that (porphinato)manganese(IV) complexes are more stable in the presence of hydroxide ion. Thus, the increase in epoxidation rate at higher aqueous acidities may result from the decrease in availability of hydroxide ion in addition to the presence of a neutral chlorine(I) species alluded to earlier.

(36) Goff, H. M.; Phillipi, M. A. *J. Am. Chem. Soc.* **1982**, *105*, 7567.

(37) (a) Spreer, L. O.; Maliyackel, A. C.; Holbrook, S.; Otvos, J. W.; Calvin, M. *J. Am. Chem. Soc.* **1986**, *108*, 1949. (b) Iwaizume, M.; Komuro, H. *Inorg. Chim. Acta* **1986**, *111*, L9.

(38) Breslow, R.; Brandl, M.; Hunger, J.; Turro, N.; Cassidy, K.; Krogh-Jespersen, K.; Westbrook, J. D. *J. Am. Chem. Soc.* **1987**, *109*, 7204.

Conclusion

Our spectroscopic evidence indicates that the major (porphinato)manganese species produced upon oxygen transfer to (tetraarylporphinato)manganese(III) complexes contain monomeric manganese(IV) centers. These complexes are $S = {}^3/_2$ spin systems and exhibit negative hyperfine shifts in their low-temperature ^2H NMR spectra. Although our spectroscopic data do not support the presence of manganese(V) complexes, we cannot discount its presence at minute concentrations in our low-temperature reaction products.

In the absence of a sixth coordinating ligand such as 4-Mepy, equilibrium concentrations of manganese(III) porphyrin π-cation radical likely react with chlorine atoms (present from homolytic bond cleavage of Cl_2 or OCl_2) to afford a reactive isoporphyrin. This complex is structurally analogous to an electrochemically produced isoporphyin but is considerably more reactive. The reactive metalloisoporphyrin effectively executes oxidative chlorination and allylic oxidation of cyclohexene. Thus, this complex is likely the species or at least one of the species responsible for the poor epoxide specificity observed in the absence of nitrogen donor ligands in the catalytic hypochlorite oxidation system.

Acknowledgment. Financial support from National Science Foundation Grant CHE 87-05703 is gratefully acknowledged. Gratitude is expressed to Professor Charles Schultz for helpful discussions regarding the ESR spectra of these complexes.

Registry No. Mn[(N-CH_3)TPP]Cl, 59765-80-9; 4-Mepy, 108-89-4; cyclohexene, 110-83-8; iodide, 20461-54-5.

Cubic, Butterfly, and Oxygen-Capped Clusters of *n*-Butyloxotin Phosphinates. A New Class of Organotin Compounds[1,2]

Robert R. Holmes,* K. C. Kumara Swamy, Charles G. Schmid,[3] and Roberta O. Day

Contribution from the Department of Chemistry, University of Massachusetts, Amherst, Massachusetts 01003. *Received February 26, 1988*

Abstract: Reaction of *n*-butylstannoic acid with the phosphinic acids, R_2PO_2H, where R = *tert*-butyl, benzyl, and cyclohexyl, has led to new types of structural forms for hexacoordinated tin: two cubic clusters, $[n\text{-BuSn(O)O}_2\text{P}(t\text{-Bu})_2]_4$ (**1**) and $[n\text{-BuSn(O)O}_2\text{P(CH}_2\text{Ph})_2]_4$ (**2**), respectively, and a "butterfly" cluster, $[n\text{-BuSn(OH)(O}_2\text{P(C}_6\text{H}_{11})_2)_2]_2$ (**3**). Interesting transformations of cubes and the butterfly derivative yield oxygen-capped cluster formulations, $[(\text{R'Sn(OH)O}_2\text{PR}_2)_3\text{O}][\text{R}_2\text{PO}_2]$, where R' = *n*-Bu and R = C_6H_{11} or CH_2Ph. ^{119}Sn and ^{31}P NMR show these structural characteristics in solution. The ^{119}Sn chemical shift correlates with increasing cluster complexity, i.e., with an increasing ligand to tin component in the various formulations discovered so far. **1** crystallizes in the triclinic space group $P\bar{1}$ with a = 13.616 (4) Å, b = 13.857 (3) Å, c = 20.544 (4) Å, α = 79.95 (2)°, β = 69.16 (2)°, γ = 71.15 (2)°, and Z = 2. **2** crystallizes in the tetragonal space group $P\bar{4}2_1c$ with a = 17.630 (4) Å, c = 11.825 (3) Å, and Z = 2. **3** crystallizes in the triclinic space group $P\bar{1}$ with a = 10.758 (3) Å, b = 12.133 (4) Å, c = 13.038 (4) Å, α = 79.93 (2)°, β = 73.72 (2)°, γ = 89.53 (2)°, and Z = 1. The conventional unweighted residuals were 0.038 (**1**), 0.042 (**2**), and 0.042 (**3**).

Our recent discovery of new structural forms of oxotin derivatives from the reaction of *n*-butylstannoic acid with phosphinic acids[1b,2,4-6] prompts us to explore the versatility of this reaction with regard to the range of possible products and their accompanying interconversions.

The reaction of monoorganostannoic acids with carboxylic acids has led to the formation of "drum" $[\text{R'Sn(O)O}_2\text{CR}]_6$[7-9] and "open-drum" (or "ladder") $[(\text{R'Sn(O)O}_2\text{CR})_2\text{R'Sn(O}_2\text{CR})_3]_2$[8,9] compositions. With phosphinic acids, a greater variety of

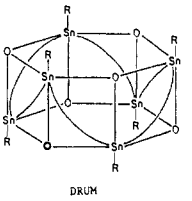

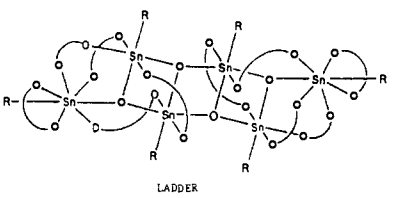

structures has been found. Although, the open-drum arrangement has yet to be observed, previous work has revealed phosphinic acids taking part in the formation of the mixed-drum composition, $[(\text{MeSn(O)O}_2\text{CMe})(\text{MeSn(O)O}_2\text{P}(t\text{-Bu})_2)]_3$,[1b] the cube formulation, $[n\text{-BuSn(O)O}_2\text{P(C}_6\text{H}_{11})_2]_4$,[4] and an oxygen-capped cluster unit, $[(n\text{-BuSn(OH)O}_2\text{PPh}_2)_3\text{O}][\text{Ph}_2\text{PO}_2]$.[5] A schematic of the latter unit illustrates its structural relationship with the drum formulation. When diphenylphosphoric acid is reacted in place of diphenylphosphinic acid, a drum $[n\text{-BuSn(O)O}_2\text{P(OPh)}_2]_6$[1b]

(1) (a) Organotin Clusters. 4. (b) Part 3: Day, R. O.; Chandrasekhar, V.; Kumara Swamy, K. C.; Holmes, J. M.; Burton, S. D.; Holmes, R. R. *Inorg. Chem.* **1988**, *27*, 2887-2893.

(2) Kumara Swamy, K. C.; Schmid, C. G.; Burton, S. D.; Nadim, H.; Day, R. O.; Holmes, R. R. *Abstracts of Papers*, 195th National Meeting of the American Chemical Society, Toronto, Canada, June 1988; American Chemical Society: Washington, DC, 1988; Abstract INOR 508.

(3) This work represents in part a portion of the Ph.D. Thesis of C. G. S., University of Massachusetts, Amherst, MA.

(4) Kumara Swamy, K. C.; Day, R. O.; Holmes, R. R. *J. Am. Chem. Soc.* **1987**, *109*, 5546-5548.

(5) Day, R. O.; Holmes, J. M.; Chandrasekhar, V.; Holmes, R. R. *J. Am. Chem. Soc.* **1987**, *109*, 940-941.

(6) Holmes, R. R.; Day, R. O.; Chandrasekhar, V.; Schmid, C. G.; Holmes, J. M. *Abstracts of Papers*, 193rd National Meeting of the American Chemical Society, Denver, CO, April 1987; American Chemical Society: Washington, DC, 1987; Abstract INOR 385.

(7) Chandrasekhar, V.; Day, R. O.; Holmes, R. R. *Inorg. Chem.* **1985**, *24*, 1970-1971.

(8) Holmes, R. R.; Schmid, C. G.; Chandrasekhar, V.; Day, R. O.; Holmes, J. M. *J. Am. Chem. Soc.* **1987**, *109*, 1408-1414.

(9) Chandrasekhar, V.; Schmid, C. G.; Burton, S. D.; Holmes, J. M.; Day, R. O.; Holmes, R. R. *Inorg. Chem.* **1987**, *26*, 1050-1056.

0002-7863/88/1510-7060$01.50/0 © 1988 American Chemical Society